Method for analyzing electron spectra observed in solar neutrino experiments

Waikwok Kwong and S. P. Rosen
Department of Physics, University of Texas at Arlington, Arlington, Texas 76019-0059
(Received 3 October 1994)

The normalized spectral ratio (the ratio of the measured electron spectrum to that of the SSM with both spectra normalized to contain the same number of events) is used to study results from electron scattering and deuterium dissociation experiments. It is found to be a very useful tool for measuring the energy-dependent deviation from the SSM and results can be expressed in terms of a single parameter—its slope. The number of events needed to see a positive slope preferred by current data at the 3σ level is about 4000–5000 for electron scattering experiments and about 2000 for deuterium dissociation experiments.

PACS number(s): 96.60.Kx, 12.15.Mm, 13.10.+q, 14.60.Pq

I. INTRODUCTION

Recoil-electron spectra observed in solar neutrino experiments can provide significant clues to the origin of the solar neutrino problem [1]. Whereas solar physics may change the normalization of these spectra, it cannot change the shapes predicted by standard solar models (SSM's) [2]. Neutrino physics can change both the normalization and the shapes, and so the observation of a change in shape is, in principle, an unambiguous signal for a neutrino physics solution rather than a solar physics one.

Unfortunately, the observed spectra are actually convolutions over the spectrum of electron neutrinos arriving at Earth and this tends to wash out the sometimes subtle differences in shape predicted by mechanisms such as the Mikheyev-Smirnov-Wolfenstein (MSW) effect [3]. Moreover, background problems restrict the observed data to the higher-energy regions of the electron spectra [4], where the differences between the SSM spectrum and other predictions are not as pronounced as in the lower-energy regions. Thus in practice deviations from SSM shapes are not easy to detect.

In this paper we wish to expand upon a method for dealing with this type of problem which was first proposed [5] in the context of the Kamiokande solar neutrino-electron scattering experiment [4]. The specific motivating issue in that case was the presence of neutral-current scattering: if electron neutrinos oscillate into other active flavors, then these flavors will scatter from electrons through neutral-current interactions alone and the corresponding cross sections will be reduced by a factor of 6 to 7. How can one determine whether such effects are present in the observed electron spectra?

The method we discussed [5] was to take the ratio of the standard model prediction to the observed spectrum *on a point-by-point basis.* If no change in shape were taking place, then this "spectral ratio" would be flat as a function of recoil-electron energy. If, on the other hand, there were a change in shape, then the spectral ratio would not be flat: its value would be much lower in regions of large changes in shape than in regions with lesser shape changes, and hence it would have an observable slope.

For example, in the nonadiabatic MSW solution [6] to the solar neutrino problem, low-energy neutrinos are much more strongly converted from electron type to other flavors and the spectral ratio would have a positive slope as a function of electron energy. By contrast, high-energy neutrinos are much more strongly converted in the adiabatic solution [7] and in this case the slope would be negative.

The situation for other models is similar. For example, with long wavelength vacuum oscillation, there is also an energy-dependent suppression like that of the MSW effect [8]; depending on the neutrino parameters, the slope of the spectral ratio can be either positive or negative. In models in which the neutrino has a large magnetic dipole moment [9], spin flips that are due solely to a magnetic field result in an energy-independent suppression and thus cannot be distinguished from the SSM by spectral analysis. When matter effects are included, the Hamiltonian of the so-called matter-enhanced spin flip has the same form as that of the MSW effect and leads to similar kind of energy-dependent suppressions. The amount of suppressions from these different mechanisms will of course be different, and the slopes of the resulting spectral ratios will not be the same.

It goes without saying that in order to apply this method successfully we need sufficient data to establish beyond any doubt that the spectral ratio is not flat. In our first work [5], we argued from an analysis of the existing spectral data from the Kamiokande II experiment [10] that approximately 3000 events would be needed in the various energy bins above 7.5 MeV. For lower thresholds, the differences between SSM and neutrino physics predictions become more pronounced and fewer events might be needed. Here we shall investigate this issue in considerable detail.

First of all, relevant experimental energy resolutions and electron detection efficiencies will be included. Secondly, we will use a new "normalized" spectral ratio in which both the experimental and the theoretical spectra are normalized to contain the same number of events.

This has the advantage of maximizing any differences between the two spectra.

Besides a more detailed analysis of solar neutrino-electron scattering, we shall also apply this normalized spectral-ratio method to the charged-current reaction $\nu + d \rightarrow 2p + e^-$ which will be observed in the SNO detector [11]. The differences between the SSM recoil-electron spectrum and, say, MSW predictions tend to be subtle and so we shall use the ratio to determine, in this case whether lower-energy electron neutrinos are being converted to other flavors and hence are losing the ability to initiate the charged-current reaction. This effect is similar to oscillations into a sterile neutrino in both Kamiokande and SNO: the neutrino is "lost" and cannot scatter even via neutral-current reactions.

We will illustrate how the normalized spectral ratio works by using the MSW solutions as an example of a model that produces energy-dependent suppressions. In Sec. II, we introduce the electron-neutrino survival probability for the MSW effect. Section III is devoted to the experimental signature for neutrino-electron scattering experiments at Kamiokande, SuperKamiokande, and SNO. The purely charged current reaction of deuterium dissociation is treated in Sec. IV. Section V contains the summary with more discussions.

II. MSW PROBABILITIES

The MSW mechanism of matter-enhanced neutrino oscillation provides us with an energy-dependent probability $P(E)$ that an electron neutrino ν_e of energy E produced in the Sun will not have oscillated into another neutrino species ν_x when it arrives at Earth. In the nonadiabatic approximation, it has a very simple form [12]:

$$P(E) = e^{-C/E} , \tag{1}$$

with

$$C = \frac{\pi \Delta m^2 \sin^2 2\theta}{4 \cos 2\theta} \left(\frac{d}{dr} \ln N_{\rm eff} \right)^{-1} . \tag{2}$$

Here, $\Delta m^2 = m(\nu_x)^2 - m(\nu_e)^2$, θ is the vacuum mixing angle between ν_e and ν_x, and $N_{\rm eff}$ is the effective density of the Sun as seen by the neutrinos with the logarithmic derivative evaluated at the resonance point.

In the adiabatic approximation, the survival probability depends on where in the Sun the neutrino is produced [13]:

$$P(E,r) = \frac{1}{2} \left(1 - \frac{p(r) \cos 2\theta}{[p^2(r) + \sin^2 2\theta]^{1/2}} \right) , \tag{3}$$

$$p(r) = 1.52 \times 10^{-7} N_{\rm eff}(r)\, E/\Delta m^2 - \cos 2\theta , \tag{4}$$

with E in MeV and Δm^2 in eV^2. Since solar neutrinos are created over a large range of density, we must average over the production point r:

$$P(E) = \int P(E,r) f(r) dr , \tag{5}$$

where $f(r)dr$ is the fraction of neutrinos produced between radius r and $r + dr$.

In the standard model, ν_x can be either ν_μ or ν_τ which we will call active neutrinos; other models may give inactive neutrinos that are undetectable on Earth, such as sterile neutrinos or unstable neutrinos which will have decayed away by the time they arrive on Earth. Sterile neutrinos differ from active and other inactive neutrinos in another aspect [14]. When ν_e oscillates into ν_μ, both neutrinos interact with the electrons and hadrons in the sun via the neutral current and this leads to an overall unobservable phase of the neutrino wave function. On the other hand, for oscillations of ν_e into a sterile neutrino, the sterile neutrino does not interact with anything as it travels through the Sun and this leads to an observable difference which is reflected in the effective density $N_{\rm eff}$ in Eqs. (2) and (4). For ν_e to ν_μ, $N_{\rm eff}$ is the electron density N_e, while for oscillations into sterile neutrinos, half the neutron density has to be taken out and $N_{\rm eff}$ becomes $N_e - N_n/2$.

This alters the point of resonance in the Sun and changes the definition of C in Eq. (2) for the two cases. However, the change in C is very small for ^{8}B neutrinos [5]. The ratio of the logarithmic derivative in (2) for sterile to active ν_x starts at 0.75 when the resonance occurs at the center of the Sun and ends at 0.989 when the resonance occurs at the surface of the Sun. The resonance for ^{8}B neutrinos typically takes place three-quarters of the way to the surface of the Sun at which point the ratio will be roughly 0.98. Therefore, for all practical purposes, we can use the same value of C for the two cases.

When solar neutrinos interact with the detector, they either produce electrons in nuclear collisions or scatter them from atomic orbits. The spectral shape of these electrons contains important information about the energy distribution of the incident neutrinos. Kamiokande is the only running experiment that measures the spectral shape directly. So far, no deviation from the SSM shape has been detected [10], mainly because of the large statistical uncertainty in the measured spectrum.

Indirect evidence for energy-dependent deviation does exist. Experiments that are sensitive to neutrinos of different energy ranges have reported different suppression factors relative to the SSM and a combined fit of the ^{37}Cl [15], Kamiokande [16], and ^{71}Ga [17,18] results performed by the GALLEX Collaboration [17] points to two small regions in the parameter space of MSW solutions: one with a small mixing angle and the other with a large mixing angle. The small angle solution is well described by the nonadiabatic approximation with $C \approx 10$; however, the more complicated adiabatic approximation must be used for the large angle solution [19].

III. NEUTRINO-ELECTRON SCATTERING EXPERIMENTS

A. Theoretical spectra

In elastic ν-e scattering, the basic cross section is given by

$$\frac{d\sigma}{dT} = \frac{G_F^2 m_e}{2\pi}\left[L_e^2 + R_e^2\left(1-\frac{T}{E}\right)^2 - R_e L_e \frac{m_e T}{E^2}\right] , \quad (6)$$

where $R_e = 2\sin^2\theta_W$ for all cases, and $L_e = R_e + 1$ for ν_e and $= R_e - 1$ for ν_μ and ν_τ; $d\sigma/dT$ is, of course, zero for sterile neutrinos.

The neutrino signal measured at Earth involves the convolution of (6) with the solar neutrino flux $\phi(E)$. When neutrino oscillations $\nu_e \leftrightarrow \nu_x$ are taken into account, the differential rate can be written as

$$\frac{dR}{dT} = \int_{E_{\min}}^{\infty} \phi(E)\left(P(E)\frac{d\sigma}{dT}(\nu_e) + [1-P(E)]\frac{d\sigma}{dT}(\nu_x)\right) dE , \quad (7)$$

where $E_{\min} = \frac{1}{2}T\,[1+(1+2m_e/T)^{1/2}]$ is the lowest energy of a neutrino that will participate in the scattering.

The results of the integral (7) using the nonadiabatic $P(E)$ of (1) have been worked out in our earlier anaylsis [5] and are reproduced here in Fig. 1. The top half shows the spectrum dR/dT for oscillations into active and inactive neutrinos. The $C = 0$ case corresponds to the SSM result where neutrinos are exactly massless and do not mix. The lower half shows the same results divided by the SSM prediction, what we called the SSM-reduced spectra. We can see that the major effect of neutrino oscillations is the reduction of the overall rate; the change in the spectral shape, although noticeable, is a much more subtle effect. A direct fit of the Kamiokande data [10] to the SSM-reduced spectra in the active case [5] gave roughly $C = 13 \pm 2$; a straight-line fit of the same data gave a slope of 0 ± 3 in units of 0.01 MeV^{-1} while the maximum slope of all the SSM-reduced spectra is only about 2 in the same unit. In essence, the SSM-reduced spectrum contains information of both the spectral shape and the overall normalization. For study of spectral shapes alone, it is more convenient to remove the overall normalization by normalizing all cases to contain the same number of events. Since the cross section is largest at low recoil energy T which is not accessible to experiments, the normalization is best done in a more realistic experimental situation.

The same results using the adiabatic probability of (3) are shown in Fig. 2. Because of the complicated dependence of $P(E)$ on both Δm^2 and $\sin^2 2\theta$, we have chosen to present results only around the large angle solution of the GALLEX fit. The spectra show negative slopes at small T, but for energies accessible to experiments, i.e., above 5 MeV, they are very flat and there will be very little observable deviation in shape from the SSM spectrum. Inclusion of experimental resolution and efficiency will only flatten these curves further. It is safe to conclude that spectral shapes cannot be used to distinguish the large angle solution from the SSM.

B. Experimental spectra

The experimental rate can be written as a function of the actual measured energy T' of the electron with the help of an energy resolution function $\rho(T,T')$ and a detection efficiency $\epsilon(T)$:

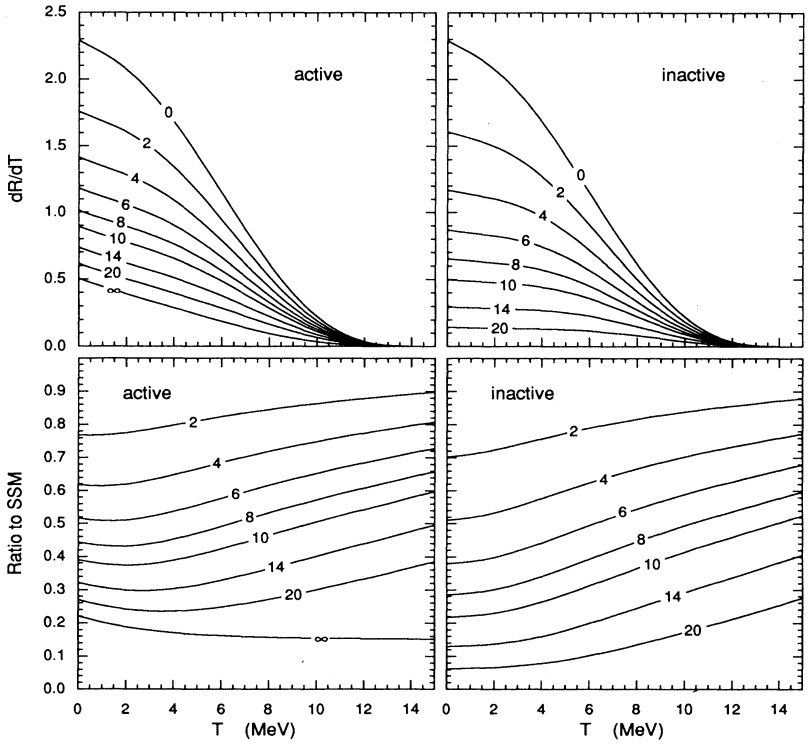

FIG. 1. Recoil spectra for electron scattering by solar ^{8}B neutrinos in the nonadiabatic approximation: The top diagrams are differential event rates and the bottom diagrams are their ratios to the corresponding SSM rate. The labels "active" and "inactive" refer to oscillations into active and inactive neutrinos, respectively. Each curve is labeled by the value of the nonadiabatic factor C.

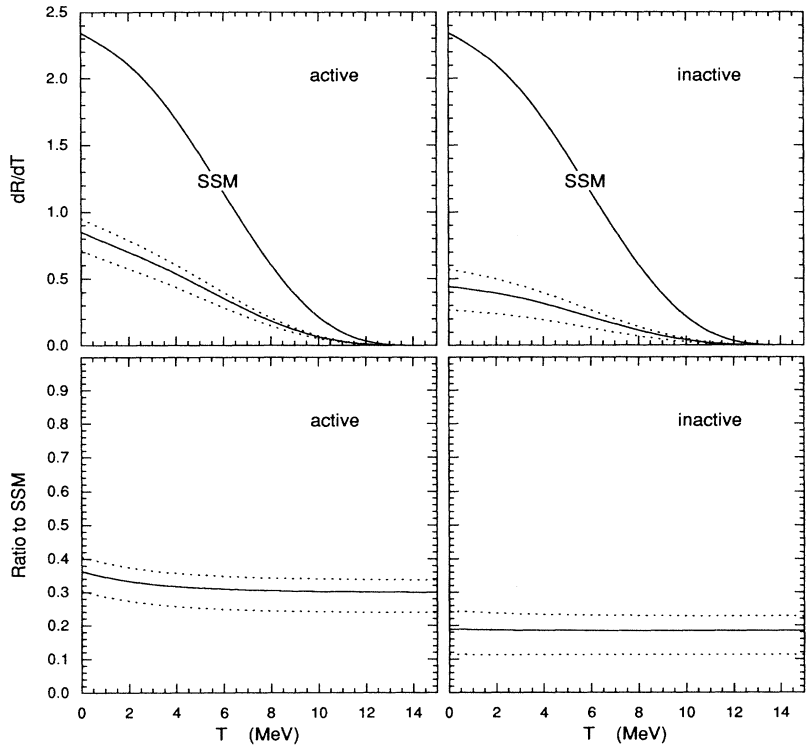

FIG. 2. Electron-recoil spectra in the adiabatic approximation near the large angle solution of the GALLEX fit. The solid curve not labeled by SSM is from the best fit with $(\sin^2 2\theta, \Delta m^2) = (0.6, 10^{-5})$. The dotted curves represent maximum 1σ deviations from the best fit. The upper and lower dotted curves have $(\sin^2 2\theta, \Delta m^2)$ values of $(0.7, 2 \times 10^{-5})$ and $(0.4, 5 \times 10^{-6})$, respectively.

$$\frac{dR'}{dT'} = \int_0^\infty \frac{dR}{dT}\, \rho(T, T')\, \epsilon(T)\, dT, \tag{8}$$

where we have used R' instead of R to distinguish it from the theoretical rate of (7). The resolution function can be approximated by [20]

$$\rho(T, T') = \frac{1}{\alpha\sqrt{2\pi}}\, e^{-(T-T')^2/2\alpha^2}\ , \tag{9}$$

with

$$\alpha(T)/T = a\sqrt{(10\ \text{MeV})/T}\ . \tag{10}$$

To simulate the Kamiokande environment we use for en-

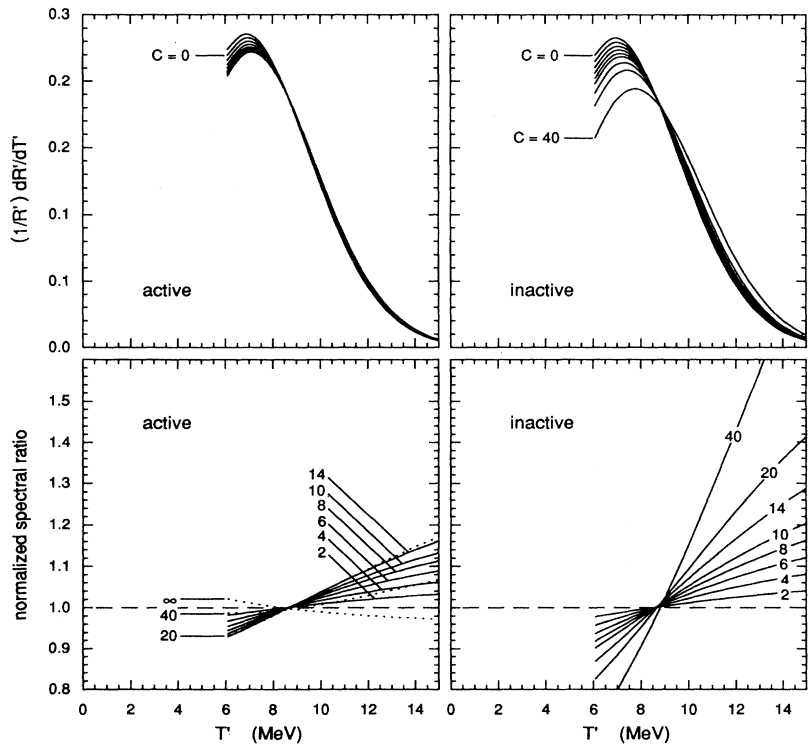

FIG. 3. Normalized nonadiabatic electron-recoil spectra for Kamiokande.

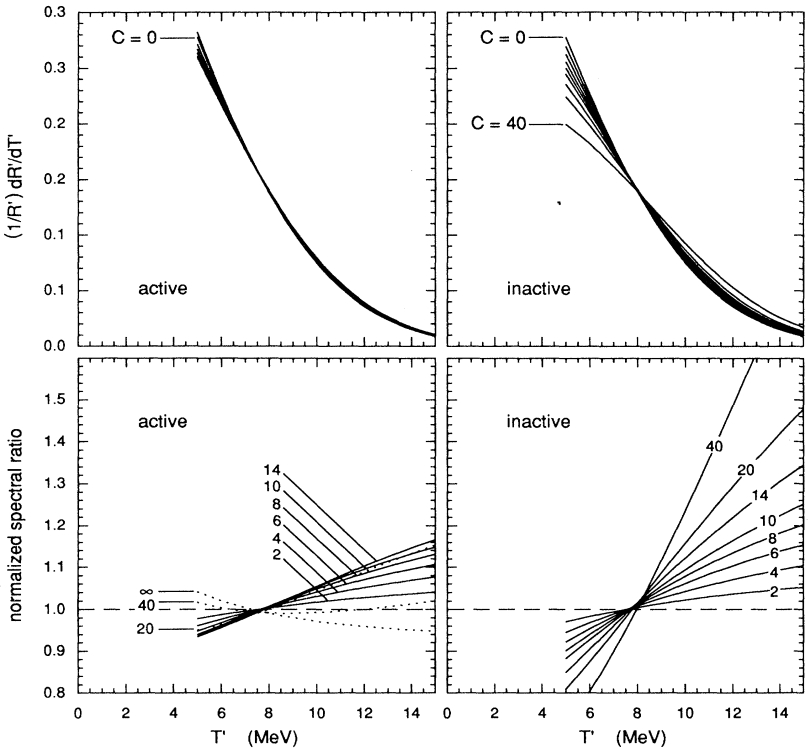

FIG. 4. Normalized nonadiabatic electron-recoil spectra for environment similar to SNO and SuperKamiokande.

ergy resolution $a = 0.2$, for detection threshold $T' \geq 6.1$ MeV, and the corresponding $\epsilon(T)$ described in [21] that has a value of 50% at threshold. Figure 3 shows the resulting nonadiabatic spectra, which are now all normalized to contain the same number of events.

For a second example, which is more relevant to SNO and SuperKamiokande [22], we use $a = 0.2\sqrt{3}$, $T' \geq 5$ MeV, and $\epsilon(T) = 100\%$. The results are shown in Fig. 4.

The same number of curves as in Fig. 1 are plotted in Figs. 3 and 4. The normalized spectra (top diagrams) for the active case are so close together that it is impossible even to label the individual curves. The improvement in resolution and efficiency for Fig. 4 does not seem to help much. If there is any measurable difference from the SSM, it will definitely not show up in such a plot. The normalized spectral ratios (to the SSM) in Figs. 3 and 4 look much better, but the actual size of the slope is still very small.

The spectra for oscillation into inactive neutrinos are somewhat more spread out than for the active case. From the spectral ratios we can see that the slopes for the inactive case do not turn over but keep increasing for

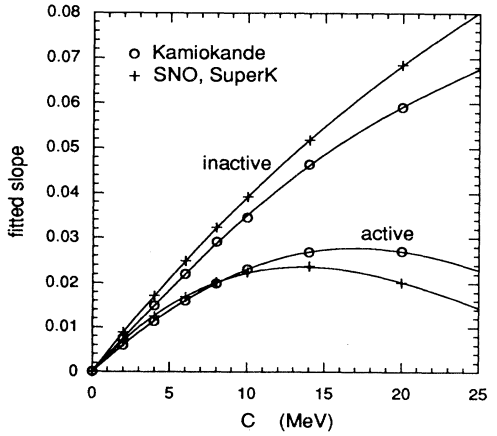

FIG. 5. Slopes of straight lines fitted to the normalized spectral ratios in Figs. 3 and 4, weighted by the number of events expected in 0.5 MeV bins.

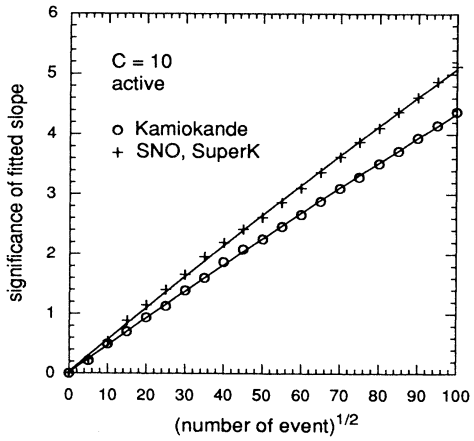

FIG. 6. Average statistical significance of the fitted slope expressed in number of standard deviations for electron scattering experiments. Uncertainties in the slopes are calculated from events generated by Monte Carlo simulations.

large value of C. This is due to the absence of neutral-current interactions for ν_x, a feature that will be shared by the deuterium dissociation experiment discussed below, and can be understood from the SSM-reduced spectra in Fig. 1: The $C = \infty$ curve corresponds to a pure neutral-current interaction and has a negative slope; the slope of the active spectral ratio must therefore turn negative at some point as C continues to increase. Without the balancing effect of the neutral current, low energy ν_e's are simply more and more efficiently converted to ν_x's, giving a steeper and steeper spectral ratio.

C. Monte Carlo simulations

To better quantify the situation, we plot in Fig. 5 the slope of a straight-line fit to the curves for the normalized spectral ratios. To simulate a real situation the spectral ratios were actually binned before being fitted. We used a 0.5 MeV bin from threshold to 16 MeV and combined the last five bins to avoid small statistics. Figure 5 shows very clearly that the inactive case always has a larger slope than the active case at the same value of C. For the active case at large C the one with the better resolution actually has a smaller slope; this is because of the lower threshold used with the improved resolution. (See Fig. 1.)

We next perform a Monte Carlo experiment to find the statistical uncertainty of these slopes. We choose the active case with $C = 10$ as a typical example and generate a total of 10 000 events according to the spectra shown in Figs. 3(a) and 4(a). The results are then binned as before and straight-line fits are performed. Figure 6 shows the average behavior of how the fitted slope improves as more events are accumulated. The case with the better resolution has indeed a better fitted slope, but the difference is modest; the main improvement will, of course, come from the much higher rate at SNO and SuperKamiokande. To reach a 3σ effect, Kamiokande needs roughly 4600 events, while SNO and SuperKamiokande will probably need 3500 events depending on the actual experimental parameters achieved.

Notice that the points in Fig. 6 do not lie on perfect straight lines; their slopes decrease slightly as the number of events increases. This is due to the error involved in approximating the normalized spectral ratios of Figs. 3 and 4 as straight lines. When this error becomes comparable to the statistical uncertainty, a direct fit to the normalized spectra for various values of C will then yield a slightly better result.

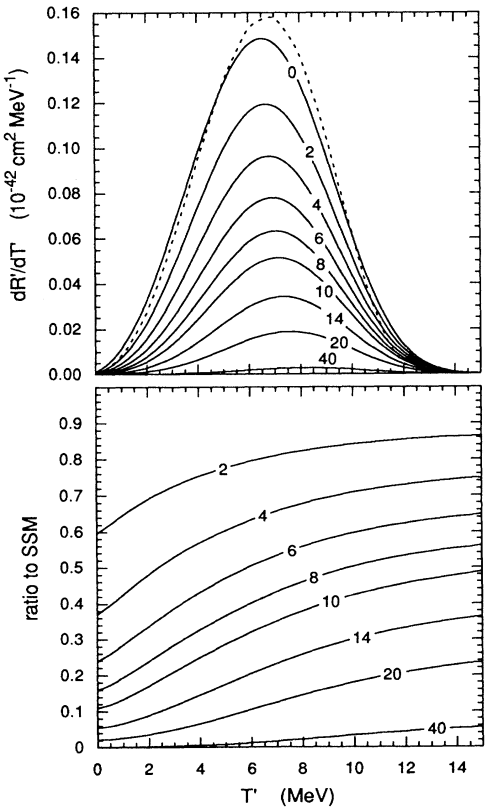

FIG. 7. Electron spectra from deuterium dissociation by ^{8}B neutrinos in the nonadiabatic approximation, experimental resolution included.

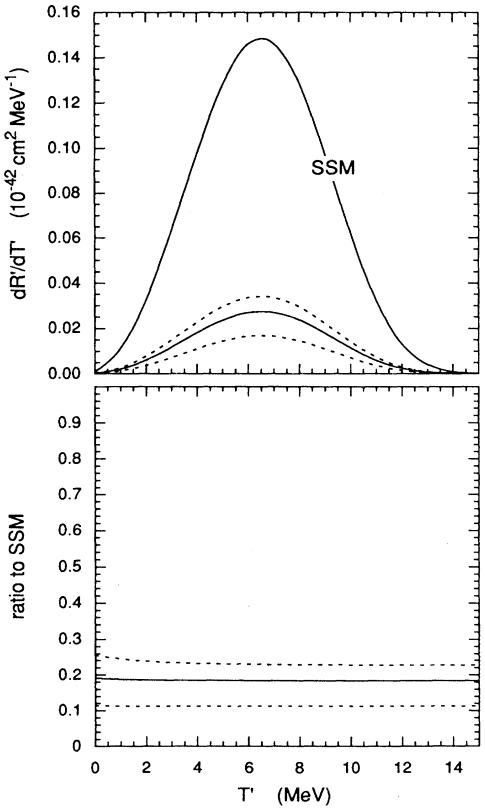

FIG. 8. Electron spectra from deuterium dissociation by ^{8}B neutrinos in the adiabatic approximation, experimental resolution included.

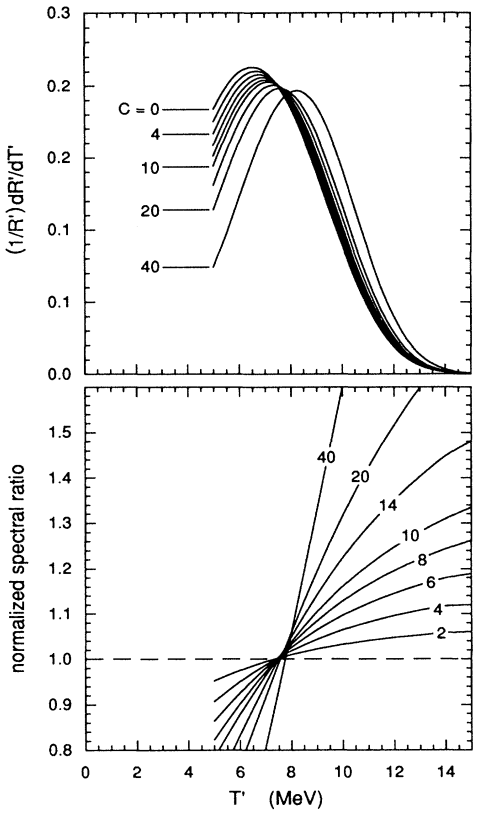

FIG. 9. Normalized nonadiabatic spectra for deuterium dissociation.

IV. NEUTRINO DISSOCIATION OF DEUTERIUM

At SNO [11], the main detection mode for solar neutrinos is via the dissociation of deuterium: $\nu + d \rightarrow 2p + e$. The outgoing electron tends to carry off most of the energy of the incident neutrino since the two-proton system has a much larger invariant mass. The resulting electron spectrum is therefore much more correlated with the neutrino energy spectrum then in the case of elastic ν-e scattering, and we expect any energy-dependent deviation from the SSM to show up more prominently than in the previous case. Furthermore, since this is a purely charged-current interaction and solar neutrinos are not energetic enough to produce muons, there will be no distinction between active and inactive neutrinos. From the discussion of the last section we anticipate that results here will resemble that of the inactive case there.

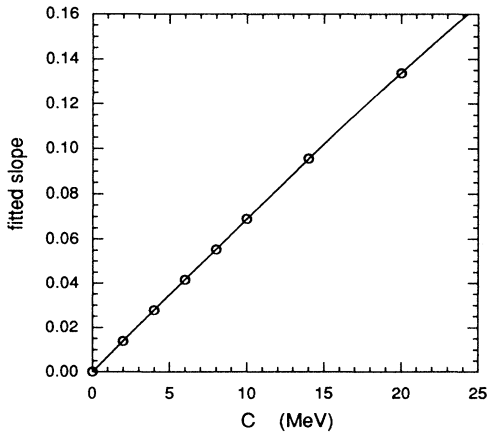

FIG. 10. Slopes of straight-line fit to the normalized spectral ratios of Fig. 9.

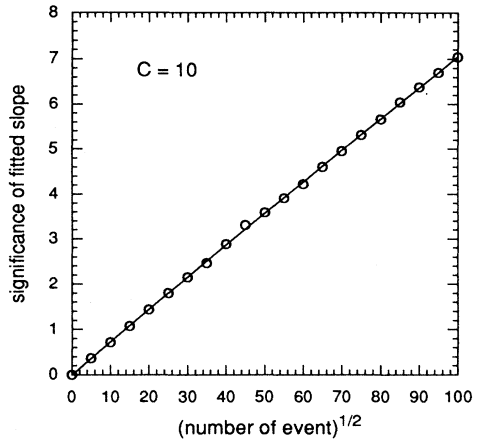

FIG. 11. Average statistical significance of the fitted slope for deuterium dissociation with errors generated by Monte Carlo simulation.

We use the simplified expression of Ref. [23] for the differential cross section. Since we are mainly concerned with ratios, the error involved will be minimal. We will use the same detector parameters from the previous section, $a = 0.2\sqrt{3}$, $T' \geq 5$ MeV, and $\epsilon = 100\%$. The theoretical spectra with experimental resolution included are shown in Figs. 7 and 8 for the nonadiabatic and adiabatic case, respectively. Again the deviation in shape from the SSM signal is extremely small near the large angle solution.

Next, we consider only the nonadiabatic case and take into account the 5 MeV threshold by normalizing all the curves in Fig. 7 to contain one event between 5 and 16 MeV. The results are plotted in Fig. 9. Figure 10 shows the fitted slopes of the spectral ratios and Fig. 11 shows the result of a Monte Carlo simulation of the $C = 10$ case for 10 000 events.

As expected, the normalized spectra are more spread out and the slopes of the spectral ratios are much larger than the previous case. We find from Fig. 11 that it takes roughly 1800 events for a 3σ effect, which is about half the numbers needed for the previous case of electron scattering.

V. SUMMARY

We have shown that the normalized spectral ratio, being independent of the total neutrino flux, is an im-

portant tool for analyzing solar neutrino data. It provides maximum sensitivity to the spectral shape without reference to any specific model and is extremely useful in distinguishing the SSM from models that produce energy-dependent suppression factors. The amount of deviation from the SSM can be measured conveniently in terms of a single parameter—the slope of the normalized spectral ratio. For the examples discussed here, the nonadiabatic MSW solution with $C \approx 10$ is presently favored by most experimental results. The amount of data needed to determine the slope for this solution at the 3σ level consists of several thousand events for electron scattering experiments (4600 for Kamiokande, 3500 for SNO and SuperKamiokande) and about 1800 events for the deuterium dissociation experiment at SNO. With SuperKamiokande alone expecting to see 8000 events a year, there should be no difficulty in establishing unequivocally a nonzero slope, if there is one. A precise measurement of model parameters such as the nonadiabatic factor C would then be possible.

Unfortunately, the normalized spectral ratio has very little sensitivity to the large angle solution of the GALLEX fit since this solution basically has the same shape as the SSM. Nevertheless, it can still be established or rejected by one of two ways. First, the overall suppression is large—it predicts 30% of the SSM flux for oscillation into ν_x that have neutral-current interactions with the detectors and 20% for those that do not—and will put severe constraints on any solar model solution. Second, its oscillation parameters fall into the same range as those which would produce a strong day-night effect due to MSW resonances inside the Earth [24] and it is close to being ruled out from the absence of a day-night effect in the Kamiokande data [25].

Finally, we would like to emphasize that here the nonadiabatic MSW solution is used mainly for the generation of a data sample for statistical analysis. Any model that produces an energy-dependent deviation from the standard spectrum will also produce a nonzero slope for the normalized spectral ratio: The ratio of two similar looking spectra with the same normalization will always lead to an approximate linear dependence on energy. At the 3σ–5σ level, i.e., before a nonzero slope can be firmly established, this is an effective way of measuring energy-dependent deviations from the standard spectrum, which is a good indication of nonstandard neutrino physics.

ACKNOWLEDGMENTS

This work is supported in part by the U.S. Department of Energy Grant No. DE-FG05-92ER40691.

[1] J. N. Bachcall, *Neutrino Astrophysics* (Cambridge University Press, Cambridge, England, 1989).
[2] J. N. Bahcall and R. Ulrich, Rev. Mod. Phys. **60**, 297 (1988); J. N. Bahcall and M. Pinsonneault, *ibid.* **64**, 885 (1992).
[3] L. Wolfenstein, Phys. Rev. D **17**, 2369 (1978); S. P. Mikheyev and A. Y. Smirnov, Nuovo Cimento C **9**, 17 (1986).
[4] K. S. Hirata *et al.*, Phys. Rev. Lett. **63**, 16 (1989); **65**, 1301 (1990); **65**, 1297 (1990); **66**, 9 (1991); Phys. Rev. D **44**, 2241 (1991).
[5] W. Kwong and S. P. Rosen, Phys. Rev. Lett. **68**, 748 (1992).
[6] S. P. Rosen and J. M. Gelb, Phys. Rev. D **34**, 969 (1986); E. W. Kolb, M. S. Turner, and T. P. Walker, Phys. Lett. B **175**, 478 (1986).
[7] H. A. Bethe, Phys. Rev. Lett. **56**, 1305 (1986).
[8] See, e.g., V. Barger, R. J. N. Phillips, and K. Whisnant, Phys. Rev. D **43**, 1110 (1991).
[9] C.-S. Lim and W. J. Marciano, Phys. Rev. D **37**, 1368 (1988); E. Kh. Akhmedov, Phys. Lett. B **213**, 64 (1988).
[10] K. S. Hirata *et al.*, Phys. Rev. Lett. **65**, 1301 (1990).
[11] D. Wark, in *Nonaccelerator Particle Physics,* Proceedings of the International Conference, Bangalore, India, 1994, edited by R. Cowsik (World Scientific, Singapore, 1994).
[12] W. C. Haxton, Phys. Rev. Lett. **57**, 1271 (1986); S. J. Parke, *ibid.* **57**, 1275 (1986).
[13] V. Barger, R. J. N. Phillips, and K. Whisnant, Phys. Rev. D **34**, 980 (1986); A. Messiah, in *'86 Massive Neutrinos in Physics and Astrophysics*, Proceedings of the 21st Rencontre de Moriond, Tignes, France, edited by O. Fackler and J. Tran Than Van (Editions Frontieres, Paris, 1986), p. 373.
[14] C.-S. Lim and W. J. Marciano, Phys. Rev. D **37**, 1368 (1988); V. Barger *et al.*, *ibid.* **43**, R1759 (1991).
[15] R. Davis, D. S. Harmer, and K. C. Hoffman, Phys. Rev. Lett. **20**, 1205 (1968); in *Proceedings of the IAU Colloquium 121 "Inside the Sun,"* Versailles, 1989, edited by G. Berthomieu and M. Cribier (Kluwer Academic, Dordrecht, in press), p. 171; in *Proceedings of the 21st International Cosmic Ray Conference*, Adelaide, Australia, 1989, edited by R. J. Protheroe (University of Adelaide, Adelaide, 1990), Vol. 12, p. 143.
[16] K. S. Hirata *et al.*, Phys. Rev. Lett. **63**, 16 (1989); **65**, 1297 (1990); Phys. Rev. D **44**, 2241 (1991).
[17] GALLEX Collaboration, P. Anselmann *et al.*, Phys. Lett. B **285**, 390 (1992).
[18] SAGE Collaboration, A. I. Abazov *et al.*, Phys. Rev. Lett. **67**, 3332 (1991).
[19] J. M. Gelb, W. Kwong, and S. P. Rosen, Phys. Rev. Lett. **69**, 1864 (1992).
[20] See, e.g., Ref. [1].
[21] K. S. Hirata *et al.*, Phys. Rev. D **44**, 2241 (1991).
[22] Z. Conner, in Proceedings of the Eighth Meeting of the Division of Particles and Fields of the American Physical Society, Albuquerque, 1994 (unpublished).
[23] F. J. Kelly and H. Überall, Phys. Rev. Lett. **16**, 145 (1966); S. D. Ellis and J. N. Bahcall, Nucl. Phys. **A114**, 636 (1968).
[24] A. J. Baltz and J. Weneser, Phys. Rev. D **35**, 528 (1987); **37**, 3364 (1988); M. Cribier *et al.*, Phys. Lett. B **182**, 89 (1986); E. D. Carlson, Phys. Rev. D **34**, 1454 (1986); A. Dar *et al.*, *ibid.* **35**, 3607 (1987).
[25] K. S. Hirata *et al.*, Phys. Rev. Lett. **66**, 9 (1991).